

# A Note on Chern-Simons Solitons

- a type III vortex from the wall vortex -

S. Bolognesi<sup>◇</sup> and S. B. Gudnason<sup>‡</sup>

<sup>◇</sup> *William I. Fine Theoretical Physics Institute, University of Minnesota,  
116 Church St. S.E., Minneapolis, MN 55455, USA*

<sup>‡</sup> *Dipartimento di Fisica, “E. Fermi”, University of Pisa, and  
Istituto Nazionale di Fisica Nucleare, Sezione di Pisa,  
Largo Pontecorvo, 3, Ed. C, 56127 Pisa, Italy*

## Abstract

We study some properties of topological Chern-Simons vortices in  $2 + 1$  dimensions. As has already been understood in the past, in the large magnetic flux limit, they are well described by a Chern-Simons domain wall, which has been compactified on a circle with the symmetric phase inside and the asymmetric phase on the outside.

Our goal is two-fold. First we want to explore how the tension depends on the magnetic flux discretized by the integer  $n$ . The BPS case is already known, but not much has been explored about the non-BPS potentials. A generic renormalizable potential has two dimensionless parameters that can be varied. Variation of only one of them lead to a type I and type II vortex, very similar to the Abrikosov-Nielsen-Olesen (ANO) case. Variation of both the parameters leads to a much richer structure. In particular we have found a new type of vortex, which is type I-like for small flux and then turns type II-like for larger flux. We could tentatively denote it a type III vortex. This results in a stable vortex with number of fluxes which can be greater than one.

Our second objective is to study the Maxwell-Chern-Simons theory and and understand how the large  $n$  limit of the CS vortex is smoothly connected with the large  $n$  limit of the ANO vortex.

June, 2008

---

<sup>◇</sup> bolognesi(at)physics.umn.edu

<sup>‡</sup> gudnason(at)df.unipi.it

# 1 Introduction

Physics in  $2 + 1$  dimensions has many interesting aspects. In particular, there is the possibility of particles carrying fractional spin and thus behaving as anyons [1]. Strictly related to the latter property it is possible, in  $2 + 1$  dimensions, to introduce a topological Chern-Simons term in the Lagrangian. The Gauss law in the presence of this term reads

$$\frac{\kappa}{2}\epsilon^{\mu\nu\rho}F_{\nu\rho} = eJ^\mu, \quad (1)$$

where  $\kappa$  is the coefficient of the Chern-Simons term. This, in particular, implies  $B = F_{12} = \frac{eJ^0}{\kappa}$ : a magnetic flux is permanently attached to a charged particle. Through the Aharonov-Bohm effect this, effectively, attaches an extra spin to charged particles. This statistical transmutation is a crucial property in the effective explanation of the fractional quantum Hall effect (FQHE). Electrons can effectively be described by bosons plus an opportune Chern-Simons interaction. Condensation leads to a superconducting quantum Hall fluid [2, 3].

Solitons, and in particular charged vortices, play an essential role in  $2 + 1$  dimensional physics and acquire interesting properties when a Chern-Simons term is present in the Lagrangian. First of all, being magnetic vortices, they also acquire an electric charge due to the Chern-Simons term. This makes them be anyons, and their semi-classical nature makes them suitable candidates to the study of anyon dynamics. They also appear as essential ingredients in the effective descriptions of the FQHE. In particular, when the magnetic field is increased between two levels of the quantum Hall fluid, vortices are created to compensate the extra magnetic field.

The literature concerning Chern-Simons solitons is quite rich. The Chern-Simons term, while not being dynamical, acquires physically different properties when coupled to different kinds of matter fields. A first obvious distinction is if the matter is relativistic or non-relativistic. The latter is certainly more appropriate when considering condensed matter phenomena. Another distinction is if the gauge group is Abelian or non-Abelian. Finally, there is also the possibility of having (or not having) the Maxwell (or Yang-Mills) term to supply kinetic properties to the gauge field. In this paper, we shall restrict ourselves to an Abelian gauge field coupled to relativistic matter, with and without the Maxwell term.

In recent works [6, 7, 8], we have considered the behavior of topological solitons, vortices and monopoles, when the magnetic flux becomes very large. Although not a priori expected, there is a simple realization of this large  $n$  limit of solitons. A domain wall appears as a sub-structure, separating an

internal phase, an unstable point of the potential where the symmetry is restored, from the external vacuum. Stabilization is achieved by a balance of energies between the magnetic flux, where the force is repulsive, and the scalar fields, for which it is attractive.

The purpose of this project is to study the large flux limit of Chern-Simons solitons and see how this is related to the previous ones. The simplest example of a self-dual Chern-Simons vortex is obtained in the so-called Chern-Simons-Higgs system. It consists of an Abelian Chern-Simons term coupled to a scalar field with a suitable sixth-order potential [9]. The potential has two degenerate vacua, one where the gauge symmetry is unbroken and one where the Higgs field acquires an expectation value. This is a basic and recurrent difference between Chern-Simons solitons and ordinary ones. In particular, there exists a domain wall separating the two vacua. The theory also admits solitons of various kinds in each vacuum, both topological and non-topological. In the large flux limit, vortices approach domain walls compactified on a circle. This has first been observed in [10].

One problem we shall consider is that of non-BPS potentials. We shall see that for particular values of the potential parameters, interesting new properties appear. In particular, there is the possibility of having a configuration where the vortex which minimizes the tension per unit flux, for certain parameters, can have an arbitrary number of fluxes and thus an arbitrary size. This is interesting, because the number of stable vortices is finite and the effective size of multiwinding vortices (or coincident vortices) hence is finite, but bigger than the classic stable 1-vortex of a (normal) type II superconductor.

Having in mind the study of the relation between the large  $n$  limit of the Maxwell vortex [7] and the Chern-Simons one [10], we proceed to consider the Maxwell-Chern-Simons model [12]. This self-dual model contains both the Maxwell and the Chern-Simons term for an Abelian gauge field. It is coupled to two scalar fields, one real and one complex. This model is particularly rich and it can, by changing the values of the parameters, interpolate between the pure Maxwell and the pure Chern-Simons theories. It is thus the right place to study the relation between the two large  $n$  limits. Even in this model, there are two degenerate vacua, one symmetric and one Higgsed. We expect that a large Maxwell-Chern-Simons vortex becomes a domain wall compactified on a circle. The matching of the large  $n$  limits of pure Maxwell and pure Chern-Simons theories will be discussed.

We have divided the paper into two sections. In the next section we first give a review of the Chern-Simons-Higgs model and then we will study the construction of the wall-vortex, that is, the large  $n$  description of the vortex in this system. In Section 3, we take into account the generalization with

the Maxwell term and study again the (expected) large  $n$  substructure of the vortex. We conclude in Section 4 and comment about possible future developments. During this project we have made extensive use of the review [13].

## 2 Abelian Chern-Simons-Higgs System

We will first make a short review of the Abelian Chern-Simons-Higgs system [9, 10] and it is obtained by combining the Abelian Chern-Simons term and a scalar Higgs field

$$\mathcal{L} = \frac{1}{4} \kappa \epsilon^{\mu\nu\rho} A_\mu F_{\nu\rho} + |D_\mu \phi|^2 - V(|\phi|) \ , \quad (2)$$

where the covariant derivative is  $D_\mu \phi = (\partial_\mu - ie A_\mu) \phi$ , the space-time metric is  $\eta_{\mu\nu} = \text{diag}(1, -1, -1)$ . The self dual potential is

$$V(|\phi|) = \frac{e^4}{\kappa^2} (|\phi|^2 - v^2)^2 |\phi|^2 \ . \quad (3)$$

The theory possesses two vacua :  $\phi = 0$  and  $|\phi| = v$ , one symmetric and one asymmetric.

The energy of the system is

$$\begin{aligned} E &= \int d^2x \left[ |D_0 \phi|^2 + |D_i \phi|^2 + V(|\phi|) \right] \ , \\ &= \int d^2x \left[ |\partial_0 \phi|^2 + \frac{\kappa^2 B^2}{4e^2 |\phi|^2} + |D_i \phi|^2 + V(|\phi|) \right] \ . \end{aligned} \quad (4)$$

The term  $\frac{\kappa^2 B^2}{4e^2 |\phi|^2}$  is fundamental, it forces the magnetic field to stay away from the  $\phi = 0$  region, that is, the magnetic field has to go to zero faster than  $|\phi|^2$ . Hence, the magnetic flux will be concentrated on the boundary between the two vacua (as it cannot sustain in the Higgs vacuum).

The equations of motion are

$$D_\mu D^\mu \phi = -\frac{\delta V}{\delta \phi^*} \ , \quad (5)$$

$$\frac{1}{2} \kappa \epsilon^{\mu\nu\rho} F_{\nu\rho} = -ie (\phi^* D^\mu \phi - \phi D^\mu \phi^*) \ . \quad (6)$$

In particular, the last equation is the Gauss law (1). The electromagnetic field is non-dynamical since there is no Maxwell term and the time component of the gauge field is thus algebraically determined

$$A_0 = -\frac{\kappa}{2e^2} \frac{F_{12}}{|\phi|^2} \ . \quad (7)$$

Hence, it will enter the Hamiltonian only through the covariant derivative.

A comment on the phases and the perturbative spectrum in the two vacua of the theory : when  $\phi = 0$ , the scalar field describes a charged particle with mass  $\mu = \frac{e^2 v^2}{\kappa}$ . The Chern-Simons term has the effect of changing the spin of these particles [9, 10, 14]. Since they have charge 1, the Gauss law implies that they have magnetic flux  $\frac{e}{\kappa}$ . The Aharonov-Bohm phase gives them an “effective” spin equal to  $\frac{e^2}{4\pi\kappa}$ . In the Higgs phase  $\phi = v$ , there is a neutral scalar particle of mass  $m \equiv \frac{2e^2 v^2}{\kappa}$ . The gauge field is massive and thus there is no effect of spin transmutation.

Performing the Bogomol’nyi factorization [5] one obtains

$$E = \int d^2x \left[ \left| D_0 \phi \pm \frac{ie^2}{\kappa} (|\phi|^2 - v^2) \phi \right|^2 + |D_{\pm} \phi|^2 \pm ev^2 B \right], \quad (8)$$

where  $D_{\pm} \phi \equiv (D_1 \pm iD_2) \phi$ . Thus, there exists the following bound on the energy

$$E \geq ev^2 |\Phi_B|, \quad (9)$$

where  $\Phi_B \equiv \int d^2x B = 2\pi n/e$  is the magnetic flux and  $n$  denotes the vortex number.

We will now describe what we are going to do. First we will review the domain wall solution that interpolates between the two vacua and subsequently the domain wall with the addition of a magnetic flux. Then in Section 2.1, we will show how the Chern-Simons vortices behave as compactified walls in the large flux limit. We shall then consider, in detail, the topological vortex and provide numerical evidence for this claim in Section 2.2. Finally, we consider the behavior of topological vortices when the potential is not the BPS one in Section 2.3.

## 2.1 The domain wall solution and the large flux limit

Now we will review the domain wall in the Chern-Simons model, first without flux and subsequently with added flux [10, 11]. The Bogomol’nyi factorization for the domain wall is

$$\begin{aligned} T &= \int dx \left[ |\partial_x \phi|^2 + \frac{e^4}{\kappa^2} (|\phi|^2 - v^2)^2 |\phi|^2 \right], \\ &= \int dx \left[ \left| \partial_x \phi \pm \frac{e^2}{\kappa} (|\phi|^2 - v^2) \phi \right|^2 \mp \frac{e^2}{2\kappa} \partial_x (|\phi|^2 - v^2)^2 \right], \end{aligned} \quad (10)$$

hence, the wall tension and the wall configuration which saturates the BPS bound read

$$T_{\text{wall}} = \frac{e^2 v^4}{2\kappa} , \quad \phi_{\text{wall}}(x) = \frac{v}{\sqrt{1 + e^{-m(x-x_0)}}} , \quad (11)$$

where  $m \equiv \frac{2e^2 v^2}{\kappa}$ .

One can add a magnetic flux to the domain wall, by switching on a gauge field  $A_y(x)$  such that  $A_y(-\infty) = -f$  and  $A_y(+\infty) = 0$ . The result is a magnetic flux density equal to  $f$  [10]. The wall tension can be rewritten as

$$T = \int dx \left[ \left| \partial_x \phi \pm \frac{e^2}{\kappa} (|\phi|^2 - v^2) \phi \right|^2 + \left| e A_y \phi \pm' \frac{\kappa}{2e} \frac{\partial_x A_y}{\phi^*} \right|^2 \mp \frac{e^2}{2\kappa} \partial_x (|\phi|^2 - v^2)^2 \mp' \frac{\kappa}{2} \partial_x (A_y^2) \right] . \quad (12)$$

The gauge field does not change the equation for the scalar field which thus remains unchanged. The second set of  $\pm$ s are independent of the first set and are thus marked with a prime. The magnetic field gives a contribution to the wall tension which now becomes<sup>1</sup>

$$T_{\text{wall+flux}} = \frac{e^2 v^4}{2\kappa} + \frac{\kappa f^2}{2} . \quad (13)$$

Having reviewed the domain wall with magnetic flux, we can now construct the Chern-Simons wall vortex as follows. We consider the compactification of the wall with flux on a circle of radius  $R$  (i.e. along the  $y$ -direction). The stabilization is achieved through a balance between the tension of the wall and the energy due to the magnetic field. We have to keep in mind that while varying the radius  $R$ , what remains constant is the total magnetic flux  $\Phi_B = 2\pi R f$ . The energy as function of the flux is thus

$$E(R) = \frac{e^2 v^4 \pi R}{\kappa} + \frac{\kappa \Phi_B^2}{4\pi R} , \quad (14)$$

and the minimization of this system gives

$$R = \frac{\kappa \Phi_B}{2\pi e v^2} = \frac{e \Phi_B}{\pi m} , \quad E = e v^2 \Phi_B . \quad (15)$$

This solution saturates the BPS bound (9) of the vortex system. This implies that in the large flux limit of the vortex, the solution should exactly become

---

<sup>1</sup> This meanwhile introduces a momentum density in the  $y$ -direction equal to  $\frac{\kappa f^2}{2}$ .

a compactified wall. A useful remark in store, is that the flux density  $f$  of the wall vortex (the compactified wall, see Fig. 1) is simply proportional to the mass: <sup>2</sup>

$$f = \frac{n}{eR} = \frac{m}{2e} . \quad (16)$$

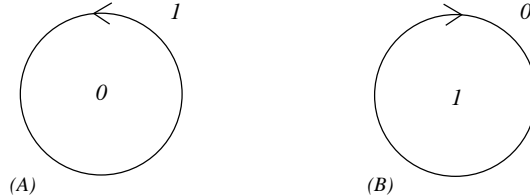


Figure 1: Schematic representation of the basic spherical symmetric solitons in the Chern-Simons-Higgs theory. They are both made of the domain wall compactified on a circle and stabilized by the angular momentum. We denote the symmetric vacuum by 0 and the asymmetric vacuum by 1. According to whether the vacuum 0 (unbroken phase) is inside or outside of the circle, we have respectively the topological vortex or the non-topological soliton of Ref. [10]. In both cases, we have chosen the orientation of the magnetic flux out of the plane (towards the reader).

## 2.2 The topological vortex in the large flux limit

Considering now the topological vortex in a cylindrical symmetric ansatz [9, 10]

$$\phi = v e^{in\theta} h(r) , \quad eA_\theta = \frac{n}{r} a(r) . \quad (17)$$

What we want to show is that the scalar field of the vortex solution for large  $n$ , simply has the profile of the domain wall (11).

The profile functions  $h(r)$  and  $a(r)$  satisfy the following boundary conditions: they both vanishes at  $r = 0$  and they both saturate at 1 for  $r \rightarrow \infty$ . After insertion of the ansatz into the BPS equations of motion (8) we get

$$\frac{\partial_r a}{r} \pm \frac{m^2}{2n} (h^2 - 1) h^2 = 0 , \quad (18)$$

$$\partial_r h \pm \frac{n}{r} (a - 1) h = 0 , \quad (19)$$

---

<sup>2</sup> A remark on the topological vortex and the non-topological soliton of Ref. [10]. The only difference is in the sign of the angular momentum which is obvious from Figure 1. The angular momentum can easily be computed to be  $J = 2\pi R^2 P$  with  $P$  the momentum density, which yields  $J = \pm \frac{\kappa}{4\pi} \Phi_B^2$ .

with  $m = \frac{2e^2v^2}{\kappa}$  as defined previously. We are looking for two boundary conditions in order to solve the problem numerically. The limiting behavior of the functions as  $r \rightarrow 0$  is

$$h = Ar^n, \quad a = \frac{m^2}{2n(2n+2)}A^2r^{2n+2}, \quad (20)$$

and in the limit  $r \rightarrow \infty$

$$h = 1 - Fe^{-mr}, \quad a = 1 - \frac{rmF}{n}e^{-mr}, \quad (21)$$

where  $A, F$  are constants.

From these equations, we can form the following boundary conditions

$$\lim_{r \rightarrow 0} \left( a - \frac{m^2 r^2}{2n(2n+2)} h^2 \right) = 0, \quad \lim_{r \rightarrow \infty} \left( a - 1 + \frac{rm}{n}(1 - h) \right) = 0. \quad (22)$$

For the numerical results we shall set the parameter  $m = 2$ , which corresponds to the choice  $e = \kappa = v = 1$ . The solution for winding number  $n = 1$  is shown in Figure 2.

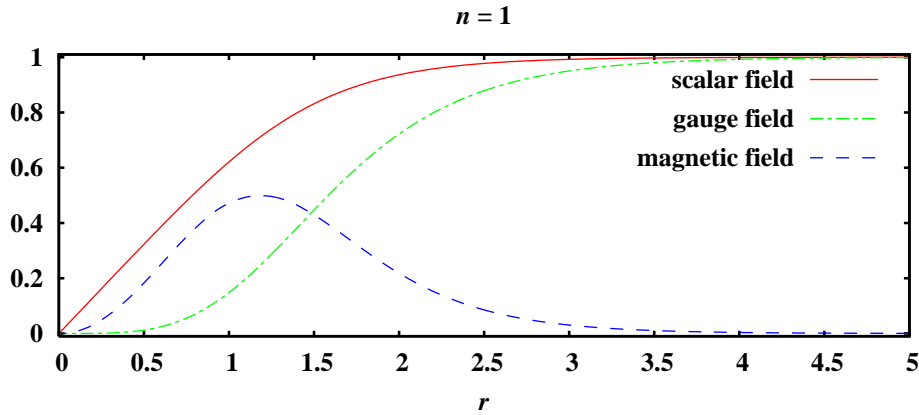


Figure 2: Profile functions for the Chern-Simons vortex with  $n = 1$ ,  $m = 2$ , where the red line (solid) is the scalar field profile, the green line (dash-dotted) is the electromagnetic potential profile (i.e.  $a(r)$  given by (17)) and the blue line (dashed) is the magnetic field. Notice that the magnetic field is already for  $n = 1$  pushed completely outside  $r = 0$  and is thus always a ring of flux placed at the vortex boundary.

We then solve the equations for various values of  $n$ . The corresponding profile functions are shown in Figure 3, 4. It is observed that the profile functions of the vortex at large  $n$  for the topological vortex are simply described



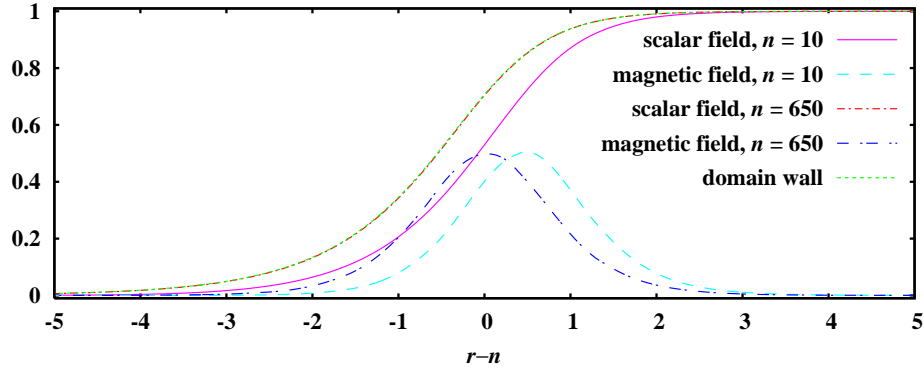


Figure 3: Profile functions for Chern-Simons vortex for various  $n$ . The radius of the vortex is  $R_{\text{vortex}} = n$  for  $m = 2$ . Notice that already for  $n = 650$ , the scalar field and the domain wall coincide.

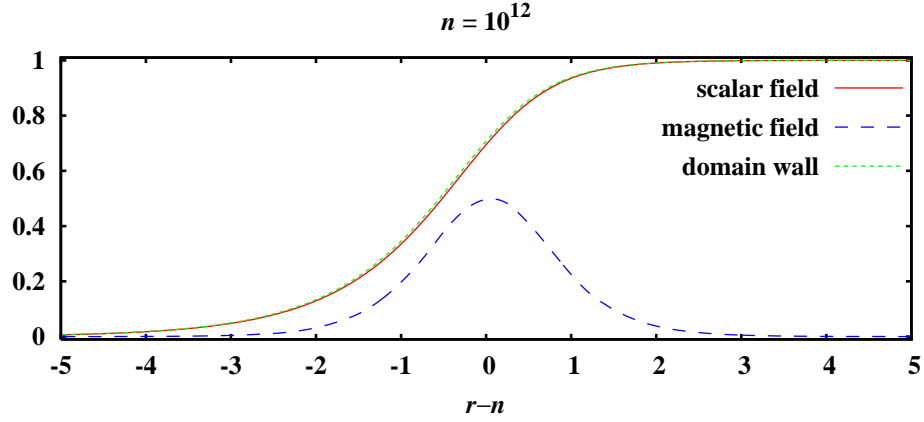


Figure 4: Profile functions for the Chern-Simons vortex for  $n = 10^{12}$ . Notice that the scalar field and the domain wall coincide.

by the profile function of the domain wall (11) situated at radius (15). The magnetic field is then simply obtained from (18).

### 2.3 Non-BPS potentials

A generic renormalizable potential in  $2 + 1$  dimensions is of sixth order, and can be parameterized by two couplings  $\alpha$  and  $\beta$

$$V(|\phi|) = \frac{\alpha e^4}{\kappa^2} (|\phi|^2 - v^2)^2 [|\phi|^2 - \beta (|\phi|^2 - v^2)] . \quad (23)$$

When  $\alpha = 1$  and  $\beta = 0$  it corresponds to the BPS potential (3). We now want to consider the Chern-Simons solitons in the case of a generic potential. We shall here concentrate on the topological vortex.

Before doing the computation we will make some qualitative remarks in order to understand what we should expect. Consider first the case  $\beta = 0$ . In this case the potential still has two degenerate vacua, we are only changing the height of the potential. The large flux limit is very useful in order to understand the qualitative behavior. In the large flux limit we still expect the vortex to become a compactified wall. The analysis of Section 2.1 should thus go through unchanged, apart from a factor of  $\sqrt{\alpha}$  in front of the wall tension.

Keeping  $\beta = 0$  and varying only  $\alpha$  should thus give a phenomenology very similar to that of the Abrikosov-Nielsen-Olesen (ANO) vortex [4]. In the large flux limit the tension is always asymptotically linear in  $n$ . Only for  $\alpha = 1$  this linear dependence is exact for all values of  $n$ . In the intermediate regime the vortices are of type I (attractive) or type II (repulsive) depending on  $\alpha$  being smaller or greater than one, respectively.

We now want to consider the case of  $\beta$  different from zero. Since we are focusing on the topological vortex, we choose  $\beta < 1$  so that the Higgs phase remains the true vacuum while the Chern-Simons phase acquires a vacuum energy density  $\varepsilon_0 = \frac{\alpha\beta e^4 v^6}{\kappa^2}$  and is metastable for  $\beta < 1/3$  and an unstable extremum otherwise.

The energy function for the compactified wall now reads

$$E(R) = T_W(\alpha, \beta)2\pi R + \frac{\kappa\Phi_B^2}{4\pi R} + \varepsilon_0\pi R^2, \quad (24)$$

where  $T_W(\alpha, \beta)$  is the domain wall tension as function of the parameter  $\alpha, \beta$ . Now to obtain the wall vortex, we have to perform a minimization with respect to the radius  $R$ , in the large  $n$  limit. We will see in a minute, that  $R$  is large in the large  $n$  limit, thus we can neglect the first term in (24) and the result is

$$R = \sqrt[3]{\frac{\kappa\Phi_B^2}{8\pi^2\varepsilon_0}}, \quad E = \frac{3}{4}\sqrt[3]{\frac{\kappa^2\varepsilon_0\Phi_B^4}{\pi}}, \quad (25)$$

which is equivalent to the vortex radius and energy in the large flux limit and furthermore, in terms of  $n$ , the radius and energy read  $R \propto n^{2/3}$  and  $E \propto n^{4/3}$ . Consistently, the radius goes as  $n^{2/3}$ , (i.e. the first term in (24) goes like  $R$  while the two remaining terms go like  $R^2$ ) and thus our previous approximation holds in the large  $n$  limit.

The equations of motion for the non-BPS Abelian Chern-Simons vortex

are

$$\partial_r^2 a - \frac{1}{r} \partial_r a - \frac{2(\partial_r a)(\partial_r h)}{h} + m^2(1-a)h^4 = 0, \quad (26)$$

$$\frac{1}{r} \partial_r (r \partial_r h) - \frac{n^2}{r^2} (1-a)^2 h + \frac{n^2 (\partial_r a)^2}{m^2 r^2 h^3} - \frac{1}{2v^2} \frac{\partial V}{\partial h} = 0. \quad (27)$$

For a generic potential we obtain

$$\frac{1}{2v^2} \frac{\partial V}{\partial h} = \frac{\alpha}{4} m^2 (h^2 - 1) [3h^2 - 3\beta(h^2 - 1) - 1] h. \quad (28)$$

In order to find numerical solutions, we need the boundary conditions at  $r \rightarrow 0$  and  $r \rightarrow \infty$ . The limiting behaviors of the profile functions are for  $r \rightarrow 0$

$$h = Ar^n, \quad a = Br^{2n+2}, \quad (29)$$

and for  $r \rightarrow \infty$

$$h = 1 - Fe^{-\sqrt{\alpha}mr}, \quad a = 1 - Ge^{-mr}. \quad (30)$$

From these behaviors we can form the following conditions

$$\lim_{r \rightarrow 0} (nh - rh') = 0, \quad \lim_{r \rightarrow 0} ((2n+2)a - ra') = 0, \quad (31)$$

$$\lim_{r \rightarrow \infty} \left( h + \frac{h'}{\sqrt{\alpha}m} \right) = 1, \quad \lim_{r \rightarrow \infty} \left( a + \frac{a'}{m} \right) = 1. \quad (32)$$

The vortex tension reads<sup>3</sup>

$$T = 2\pi v^2 \int dr r \left\{ \frac{n^2}{m^2} \frac{(\partial_r a)^2}{r^2 h^2} + (\partial_r h)^2 + \frac{n^2}{r^2} (1-a)^2 h^2 + \frac{\alpha}{4} m^2 (h^2 - 1)^2 [h^2 - \beta(h^2 - 1)] \right\}. \quad (33)$$

First, we study numerically the system with  $\beta = 0$ . The energy function of the compactified wall will, however, change with respect to (24) and (25) because of zero  $\varepsilon_0$  and it is

$$E(R) = \frac{\sqrt{\alpha} e^2 v^4 \pi R}{\kappa} + \frac{\kappa \Phi_B^2}{4\pi R}, \quad (34)$$

which gives a radius and energy in the large flux limit of respectively

$$R = \frac{\kappa \Phi_B}{\sqrt[4]{\alpha} 2\pi e v^2}, \quad E = \sqrt[4]{\alpha} e v^2 \Phi_B. \quad (35)$$

---

<sup>3</sup>Notice that in our abuse of notation, the tension is a 1-dimensional integral for the wall and 2-dimensional integral for the vortex.

In the large flux limit, we can calculate the profile function for the scalar field and the gauge field analytically, using the 1 + 1 dimensional system (the domain wall)

$$\lim_{n \rightarrow \infty} h = \frac{1}{\sqrt{1 + e^{-\sqrt{\alpha}m(x-x_0)}}}, \quad \lim_{n \rightarrow \infty} a = \frac{e^{m(x-x_0)}}{\left[1 + e^{\sqrt{\alpha}m(x-x_0)}\right]^{\frac{1}{\sqrt{\alpha}}}}. \quad (36)$$

We find exact agreement of the numerical integrated profile functions for large values of  $n$  with the above results; the vortex becomes a compactified wall in the large  $n$  limit.

In Figure 5 is shown the vortex tension normalized for convenience by a numerical factor and  $\sqrt[4]{\alpha}$ , which puts the different vortex tensions on equal footing at large  $n$ . We denote by  $\mathcal{T} \equiv \frac{T}{n}$  the vortex tension per unit flux.

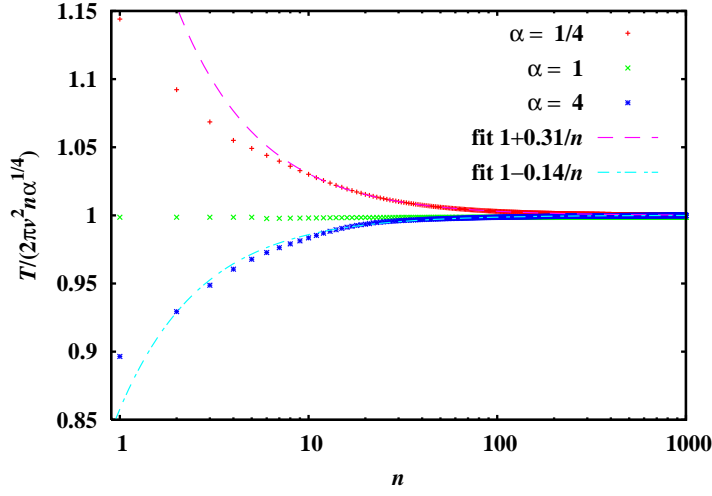


Figure 5: Vortex tension divided by  $2\pi v^2 \sqrt[4]{\alpha} n$  as function of the winding number  $n$ , for various values of  $\alpha$ ;  $1/4, 1, 4$ , corresponding to a type I, a BPS and a type II vortex.  $1/n$  fits of the non-BPS vortex tensions are shown and are seen to match reasonably at large  $n$ .

The curves for the vortex tension per unit flux  $\mathcal{T}$  approach the large flux limit value (i.e.  $2\pi v^2 \sqrt[4]{\alpha}$ ) approximately as  $1/n$  (see Figure 5).

We will now turn to the generic case with  $\beta \neq 0$ . In terms of  $n$ , the vortex tension per unit flux  $\mathcal{T}$  will go as  $n^{\frac{1}{3}}$  in the large flux limit. First a word of our expectations. We seek to combine the type I vortex behavior at small  $n$  (attractive force) with the large  $n$  behavior due to the presence of a non-zero vacuum energy density  $\varepsilon_0 = \frac{\alpha\beta e^4 v^6}{\kappa^2}$ . Naively, this gives an attractive force for

small  $n$  and a repulsive force for large  $n$  and thus a vortex with finite units of flux greater than one (finite size) as the ones with additional flux will decay.

In Figure 6, we show the vortex tension per unit of flux for a type I ( $\alpha < 1$ ) vortex with  $\alpha = \frac{1}{128}$  where we switch on a small  $\beta = 0.03$ . For this value of  $\beta$ , the Chern-Simons vacuum is metastable.

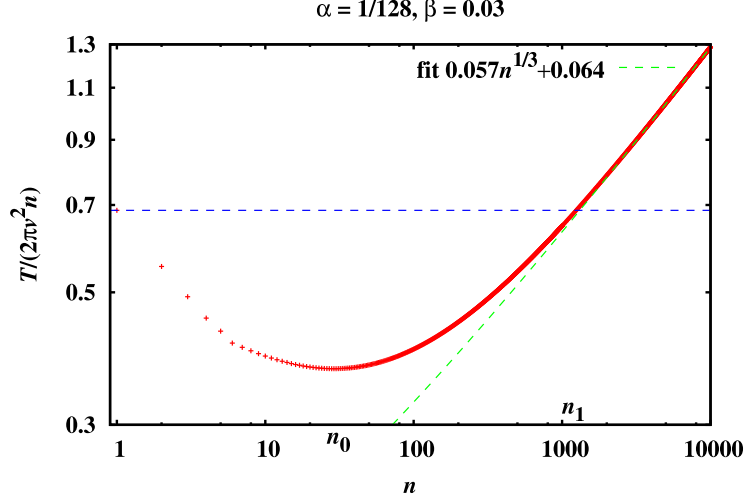


Figure 6: Vortex tension divided by  $2\pi v^2 n$  as function of the winding number  $n$ , for a vortex with  $\alpha = \frac{1}{128}$  and  $\beta = 0.03$ . The large  $n$  behavior is as predicted proportional to  $n^{\frac{1}{3}}$  and the small  $n$  behavior is type I-like, thus we have found a vortex with attractive force for small  $n$  and repulsive force for large  $n$ . We could tentatively denote it a type III vortex.  $n_0$  denotes the winding number with the minimal vortex tension.

From the figure we can define three domains

$$\begin{aligned}
 A : & 1 < n \leq n_0, \text{ where } T(n_0) < T(n), \forall n \neq n_0, \\
 B : & n_0 < n < n_1, \text{ where } n_1 \equiv \left\{ n' \in \mathbb{Z}_+ \mid \min \left( \frac{T(n')}{n'} \right) \geq T(1) \right\}, \\
 C : & n_1 \leq n,
 \end{aligned} \tag{37}$$

where we have assumed no degeneracy of the lowest tension state. Considering first the domain  $A$ , we can prove stability as follows  $T(2) < 2T(1)$ , is stable;  $T(3) < 3T(1)$ , and  $\frac{T(3)}{3} < \frac{T(2)}{2} \Rightarrow T(3) < T(2) + \frac{T(2)}{2} < T(2) + T(1)$ , thus it is stable in all channels.

Generically

$$\begin{aligned}
T(n+m) &< T(n) + \frac{m}{n}T(n) , \text{ for } n+m \leq n_0 , \\
&< T(n) + mT(1) , \\
&< T(n) + T(m) , \quad \text{for } , m \leq n ,
\end{aligned} \tag{38}$$

where  $n, m \in \mathbb{Z}_+$ . Hence, by induction it is seen that the vortices in domain  $A$  are stable to decay in any channel.

In domain  $C$  it is trivially shown that all vortices are unstable to decay into 1-vortices :  $T(n) > nT(1)$ ,  $\forall n \geq n_1$ .

In domain  $B$  it is a priori not so easy to see which channels are allowed and depends on the numerics. In general, the vortices will be unstable to decay in some channels, but it is not certain that there cannot be stable vortices here. We can comment on special points which are instable, that is, one can easily show that  $T(rn_0) > rT(n_0)$ ,  $r \in \mathbb{Z}_+$ , however, these windings might be larger than  $n_1$ .

The upshot is to note that for small  $\alpha$  and  $\beta$ , there will exist a “fat” (winding  $> 1$ ) vortex with a finite winding number  $n_0$  which is stable and preferred energetically and above a certain winding number larger than  $n_0$  the vortices will decay. This means that vortices will attract to some certain finite size and could be detectable in certain kinds of superconductors and superfluids in 2 dimensional systems. In other words, the vortices are attractive until they reach a critical size and then from that point they will repel additional fluxes. Hence, it is type I at first and when flux adds up, it turns into type II, we could denote this behavior a type III vortex.<sup>4</sup>

We explore now an approximate behavior of the function  $n_0(\alpha, \beta)$ . In Figure 7, we show the winding number  $n_0$  where the vortex has minimal vortex tension per unit flux (see Figure 6). In the top-most panel is shown  $n_0$  as function of  $\beta$  for fixed  $\alpha = 1/128$  and in the bottom-most panel,  $n_0$  as function of  $\alpha$  for fixed  $\beta = 0.03$ . In both figures, we have made a fit valid for small values of  $\beta, \alpha$ , respectively.

Around the point  $(\frac{1}{128}, 0.03)$  in  $(\alpha, \beta)$ -space, we can from the fits guess the following approximate formula, which is only valid for small couplings (as the effect is terminated when  $\alpha \sim \alpha_{\text{critical}}$  or  $\beta \sim \beta_{\text{critical}}$  i.e.  $n_0$  becomes equal to one)

$$n_0 \sim \frac{C}{\alpha^{\frac{11}{40}}\beta} , \tag{39}$$

---

<sup>4</sup>In non-Abelian non-BPS theories there are more possibilities as the forces in general have dependence on the internal properties of such systems. Recently, it was shown [15] that such a non-Abelian vortex in an Extended-Abelian-Higgs theory can have a distance dependent force which turns from attractive to repulsive at some distance.

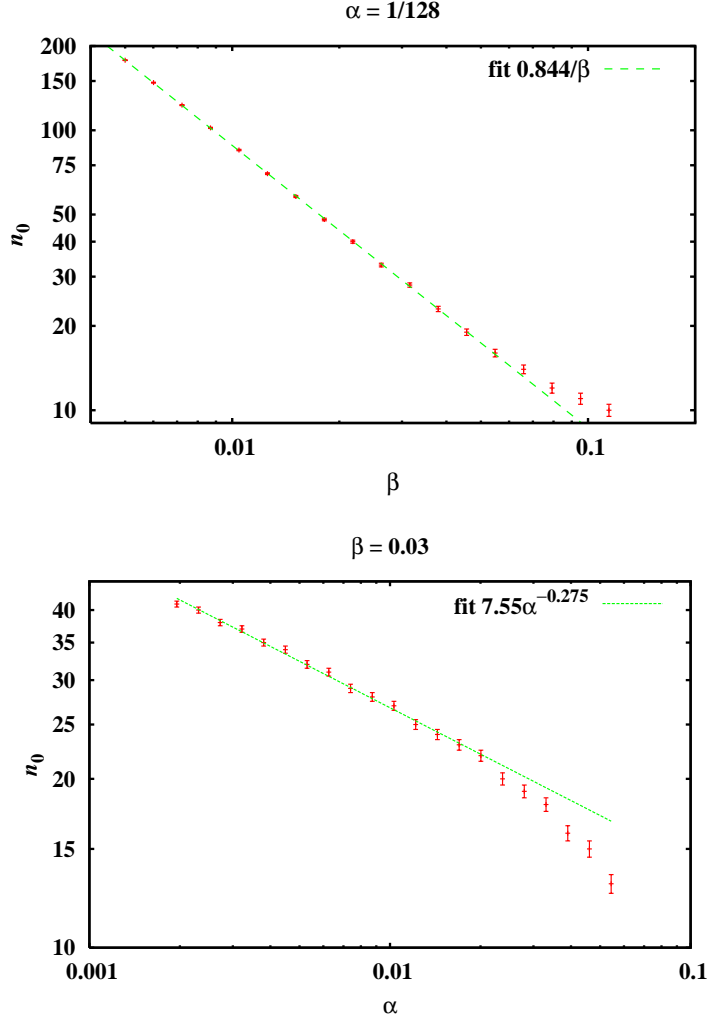


Figure 7: The winding number  $n_0$  where the vortex has minimal vortex tension per unit flux  $\mathcal{T}$ . *Top panel:*  $n_0$  as function of the coupling  $\beta$  for fixed coupling  $\alpha = \frac{1}{128}$ . For small  $\beta$  ( $\beta \lesssim 0.05$ ), the fit shows that  $n_0$  scales quite well proportional to  $\frac{1}{\beta}$ . Note that the potential is such that the Chern-Simons vacuum becomes unstable for  $\beta \geq \frac{1}{3}$ . *Bottom panel:*  $n_0$  as function of the coupling  $\alpha$  for fixed coupling  $\beta = 0.03$ . For small  $\alpha$  ( $\alpha \lesssim 0.02$ ), the fit shows good scaling proportional to  $\alpha^{-\frac{11}{40}}$ . The error-bars are simply a reminder that the function  $n_0 \in \mathbb{Z}$ .

where the constant is  $C \sim 0.22$ . We have found  $\alpha_{\text{critical}}$  and  $\beta_{\text{critical}}$  to be less than one but of order  $\mathcal{O}(10^{-1})$ . It could be interesting to see how these functions :  $\alpha_{\text{critical}}(\beta), \beta_{\text{critical}}(\alpha)$  behave, but would require a better understanding of the effects coming to play at large couplings.

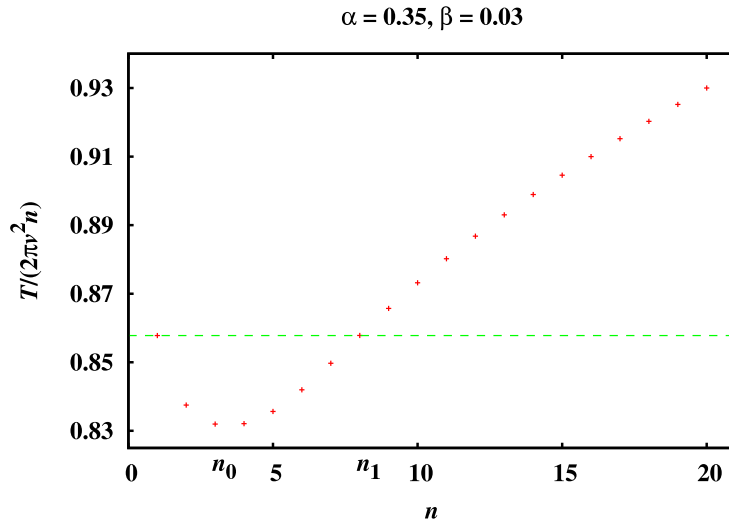


Figure 8: Vortex tension divided by  $2\pi v^2 n$  as function of the winding number  $n$ , for a vortex with  $\alpha = 0.35$  and  $\beta = 0.03$ . The couplings are tuned in such away that  $n_0$ , the winding with minimal vortex tension per unit flux, is very small (here  $n_0 = 3$ ). Thus the optimal size, energetically, is quite small, but still bigger than the 1-vortex. A simple calculation shows that all vortices with  $n > 4$  are unstable to decay.

For phenomenological considerations, it would be interesting to tune  $n_0$  to some small value. As  $n_0$  approaches infinitely large values, the superconductor is effectively of type I and the flux will break the superconducting phase. We expect more than a single point in  $(\alpha, \beta)$ -space to satisfy this condition, actually a line (region) near the critical border :  $\alpha(\beta) \lesssim \alpha_{\text{critical}}(\beta)$  or equivalently  $\beta(\alpha) \lesssim \beta_{\text{critical}}(\alpha)$ . In Figure 8 is shown such a configuration where we have tuned the parameters as :  $\alpha = 0.35$  and  $\beta = 0.03$ .

We think that this object could be detectable in 2-dimensional superconductors in the laboratory, at least in principle.

### 3 Abelian Maxwell-Chern-Simons System

Adding a Maxwell term to the Chern-Simons Lagrangian, we have a richer system which will contain both Abrikosov-Nielsen-Olesen (ANO) vortices and Chern-Simons vortices in respective limits of the coupling constants [12]. First we will make a short review of the model and then construct the domain wall and then use the latter to study the vortex in the large flux limit.



The self-dual Maxwell-Chern-Simons Lagrangian is [12]

$$\begin{aligned}\mathcal{L} = & -\frac{1}{4}F_{\mu\nu}F^{\mu\nu} + \frac{1}{4}\kappa\epsilon^{\mu\nu\rho}A_\mu F_{\nu\rho} \\ & + |D_\mu\phi|^2 + \frac{1}{2}(\partial_\mu N)^2 - U_{\text{BPS}}(|\phi|, N) \ ,\end{aligned}\quad (40)$$

where the BPS potential reads

$$U_{\text{BPS}}(|\phi|, N) = \frac{1}{2} [e|\phi|^2 + \kappa N - ev^2]^2 + e^2 N^2 |\phi|^2 \ . \quad (41)$$

Note that in order to obtain a self-dual theory, we have to introduce a neutral real scalar field  $N$ . The interesting point to note about this theory is that it reduces to the Abelian-Higgs theory and the Chern-Simons theory in respective limits of the couplings  $e, \kappa$ .

The theory has two degenerate vacua; a symmetric one where  $\phi = 0$  and  $N = \frac{ev^2}{\kappa}$  and an asymmetric one where  $|\phi| = v$  and  $N = 0$ . Topological solitons exist in the asymmetric phase and so-called non-topological solitons exist in the symmetric phase, see e.g. ref. [12]. In order to see that the system reduces correctly to the two theories, one can perform the Bogomol'nyi completion of the energy

$$\begin{aligned}E = \int d^2x \left\{ \frac{1}{2}(F_{i0} \pm \partial_i N)^2 + \frac{1}{2}(F_{12} \pm (e|\phi|^2 + \kappa N - ev^2))^2 \right. \\ \left. + |D_0\phi \mp ie\phi N|^2 + |D_\pm\phi|^2 + \frac{1}{2}(\partial_0 N)^2 \right\} \pm ev^2\Phi_B \ ,\end{aligned}\quad (42)$$

from which the self-duality equations are obtained

$$D_\pm\phi = 0 \ , \quad (43)$$

$$F_{12} \pm (e|\phi|^2 - ev^2 + \kappa N) = 0 \ , \quad (44)$$

where  $A_0 = \mp N$  solves two of the four BPS equations. There are too many degrees of freedom in this system and it needs to be accompanied by the Gauss law, which is simply the variation of the Lagrangian (40) with respect to  $A_0$

$$-\partial_i F_{i0} + \kappa F_{12} + ie[\phi^* D_0\phi - \phi(D_0\phi)^*] = 0 \ . \quad (45)$$

It is noteworthy to remark that the equation which in the Chern-Simons case was just algebraic has now become a differential equation.

Back to the two mentioned limits of this theory, it is now easy to see that the system of BPS equations (43),(44) reduces to that of the Abelian-Higgs

model by setting  $\kappa = 0$ , which in turn allows us to set  $A_0 = N = 0$  and the second BPS equation reads

$$F_{12} \pm e (|\phi|^2 - v^2) = 0 . \quad (46)$$

Taking now the other limit i.e.  $\kappa \rightarrow \infty$  while holding  $\frac{e^2}{\kappa}$  fixed, the second derivative in the Gauss law (45) is eliminated and the Gauss law constraint is the well-known algebraic expression of the Chern-Simons theory (7). Henceforth, it is straightforward to find that the second BPS equation is

$$F_{12} \pm \frac{2e^3}{\kappa^2} (|\phi|^2 - v^2) |\phi|^2 = 0 . \quad (47)$$

Our immediate aim is to consider the large flux limit of this system. For the existence of two vacua, it is natural to conjecture that the compactified domain wall shall be the solution for a large flux soliton. But what we are particularly interested in, is the matching of the large- $n$  ANO vortex with the large- $n$  Chern-Simons vortex. We clearly expect a smooth interpolation between these systems also to be present in the large flux limit.

Due to the apparent complexity of the system (four degrees of freedom), from a numerical point of view, we take as a conjecture that also this system will be well described by a domain wall interpolating the two vacua: the symmetric and the asymmetric one, being compactified on a circle. Thus for the topological vortex, which we consider now, the symmetric vacuum will be enclosed inside the wall and the asymmetric left outside. Therefore we will study the Maxwell-Chern-Simons domain wall in the next Subsection.

### 3.1 Domain wall

Considering a dimensional reduction of the system (40), we find the domain wall energy

$$\begin{aligned} T &= \int dx \left[ |\partial_x \phi|^2 + \frac{1}{2} (\partial_x N)^2 + U_{\text{BPS}}(|\phi|, N) \right] , \\ &= \int dx \left[ |\partial_x \phi \pm eN\phi|^2 + \frac{1}{2} (\partial_x N \pm (e|\phi|^2 + \kappa N - ev^2))^2 \right. \\ &\quad \left. \mp \partial_x \left( eN|\phi|^2 + \frac{1}{2} \kappa N^2 - ev^2 N \right) \right] , \end{aligned} \quad (48)$$

from which the tension of the wall (when it is BPS saturated) can be read off the total derivative term to be

$$T_{\text{wall}} = \frac{e^2 v^4}{2\kappa} . \quad (49)$$

It would be interesting to add flux to the wall, analogously to the Chern-Simons wall considered previously. We take the energy stemming from the system (40) with the gauge fields turned on.  $A_x$  turns out to be zero in the BPS wall and the energy reads

$$\begin{aligned}
T &= \int dx \left[ |\partial_x \phi|^2 + \frac{1}{2} (\partial_x N)^2 + U_{\text{BPS}}(|\phi|, N) \right. \\
&\quad \left. + \frac{1}{2} (\partial_x A_0)^2 + \frac{1}{2} (\partial_x A_y)^2 + e^2 A_0^2 |\phi|^2 + e^2 A_y^2 |\phi|^2 \right] , \\
&= \int dx \left[ |\partial_x \phi \pm eN\phi|^2 + \frac{1}{2} (\partial_x N \pm (e|\phi|^2 + \kappa N - ev^2))^2 \right. \\
&\quad \mp \partial_x \left( eN|\phi|^2 + \frac{1}{2} \kappa N^2 - ev^2 N \right) + \frac{1}{2} (\partial_x A_0 \pm' \partial_x A_y)^2 \\
&\quad \left. + ((A_0 \pm' A_y)e|\phi|)^2 \mp' \partial_x \left( A_y \partial_x A_0 - \frac{1}{2} \kappa A_y^2 \right) \right] , \tag{50}
\end{aligned}$$

where the Gauss law has been used in writing the Bogomol'nyi completion and the second set of  $\pm$ s is independent of the first set and thus is marked with a prime. If we now consider a flux analogous to the previous case of the Chern-Simons wall, i.e.  $A_y(-\infty) = -f$  and  $A_y(+\infty) = 0$  and furthermore  $\partial_x A_y(\pm\infty) = 0$ . The wall tension changes according to

$$T_{\text{wall+flux}} = \frac{e^2 v^4}{2\kappa} + \frac{\kappa f^2}{2} . \tag{51}$$

Notice that the tension coincides with that of the Chern-Simons wall (13).

From the tension (50) we can read off the BPS equations of motion. Firstly, we notice the triviality of the flux equations which simply imply  $A_0 = \mp A_y$ . From the scalars, on the other hand, there is interesting information to gather

$$\Xi = \mp \frac{\kappa}{e} \partial_x \chi , \tag{52}$$

$$\partial_x^2 \chi \pm \kappa \partial_x \chi - e^2 v^2 (e^{2\chi} - 1) = 0 , \tag{53}$$

where  $\chi = \log\left(\frac{|\phi|}{v}\right)$  and  $\Xi = \kappa N$ . Let us first look at the limits of the wall. Taking  $\kappa \rightarrow \infty$  holding  $\frac{e^2}{\kappa}$  fixed, we readily obtain exactly the Chern-Simons wall (10). Taking now  $\kappa \rightarrow 0$  we see the system is governed by the mass-squared  $e^2 v^2$  which stems from the Abelian-Higgs system.

We now are now settled to solve the domain wall (53) numerically. The scalar field  $N$  is readily obtained from (52) and the magnetic field has to be obtained by the Gauss law (45) with  $A_0 = A_y$ . It is noteworthy to

remark that the vorticity of the uncompactified wall is not fixed a priori, so a rescaling of the magnetic field is a degree freedom of this system. However, upon compactification for obtaining the wall vortex, the flux density is simply  $f = \frac{m}{2e}$  as was computed for the Chern-Simons domain wall (16). Hence, the vorticity is given in the large flux limit and is not a free parameter.

Looking ahead of view, we also know that the BPS equations for the vortex system should be obeyed for the vortex, which in the large flux limit looks like a wall, and we could make the crude guess to use the equation for the magnetic field (44), which is purely algebraic. We find that the result coincides with the integration of the Gauss law, up to an overall factor, but this simply fixes correctly the vorticity such that (16) is obeyed.

The numerical results are shown in Figures 9, 10 and 11. We start by entering the scene with couplings  $e = \kappa = 1$  and we notice a Chern-Simons-like behavior of the fields: the magnetic field is trapped in the wall. Keeping the electric charge fixed and decreasing the Chern-Simons coupling  $\kappa$  we observe that the magnetic field crawls inside the wall, i.e. to the side of the symmetric phase. This is expected, as the magnetic flux is captured inside the ANO vortex, and we expect to see a plateau rising as  $\kappa$  goes to zero. Taking a look at the left hand side graph of Figure 11, we see that some plateau is forming, but the field  $\Xi = \kappa N$  wants to get back to its VEV, which is  $ev^2$  (here  $\langle \Xi \rangle = 1$ ). As  $\kappa$  is sent to zero the VEV of  $\Xi$  is pushed away to infinity and the ANO wall vortex has emerged. Note that the energy is infinite, unless the wall is compactified on a circle.

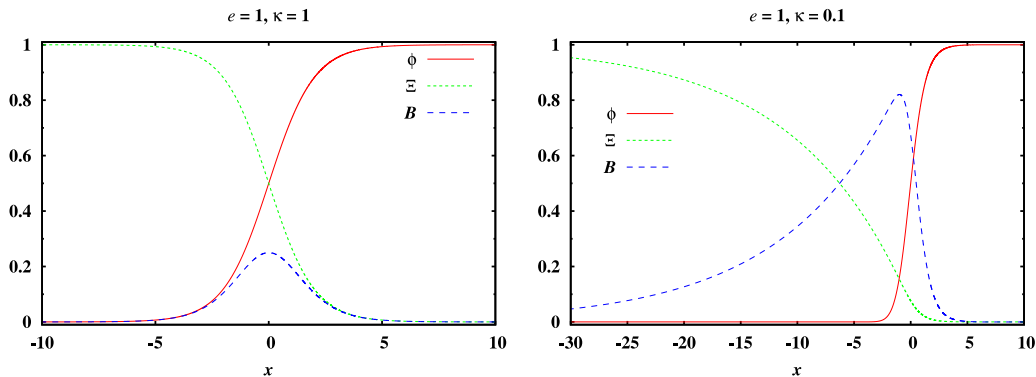


Figure 9: The fields of the Maxwell-Chern-Simons domain wall with corresponding magnetic field properly normalized. Left panel:  $e = 1, \kappa = 1$ . Right panel:  $e = 1, \kappa = 0.1$ . Notice how the magnetic field starts to be pushed “inside” the domain wall (inside means inside the wall vortex, when one considers a compactification of the domain wall on a circle).

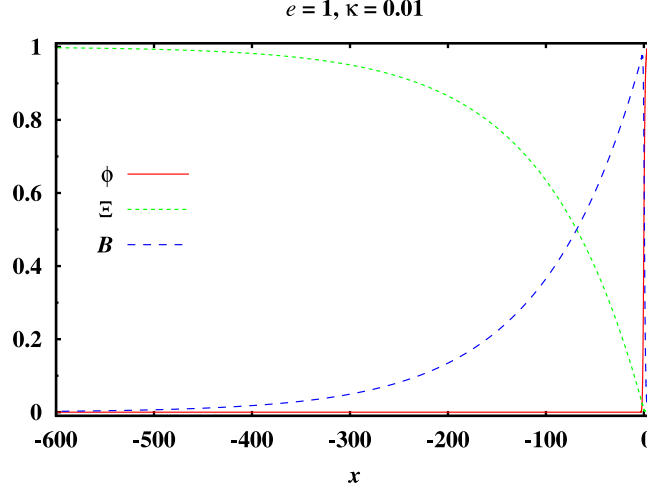


Figure 10: The tails of the fields of the Maxwell-Chern-Simons domain wall for  $e = 1, \kappa = 0.01$  with corresponding magnetic field properly normalized. Solving the BPS equation for  $N$  from (50) with  $\phi = 0$  we obtain the tail (which means far to the left of the wall) of the field  $N \sim \frac{ev^2}{\kappa} (1 - e^{\kappa x})$  and thus the tail of the magnetic field goes like  $B \sim ev^2 e^{\kappa x}$ .

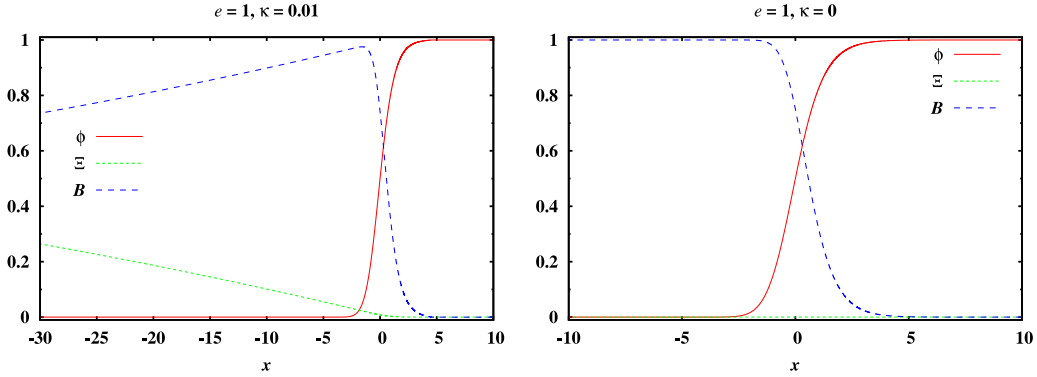


Figure 11: The fields of the Maxwell-Chern-Simons domain wall with corresponding magnetic field properly normalized. Left panel:  $e = 1, \kappa = 0.01$ . Right panel:  $e = 1, \kappa = 0$ . Notice how the field  $\Xi$  goes slowly towards its VEV (here  $\langle \Xi \rangle = 1$ ) and then for  $\kappa \rightarrow 0$  the VEV is pushed off to infinity and the Coulomb phase can persist inside the wall vortex.

### 3.2 In the large $n$ limit of the vortex: interpolation between ANO type and CS type

Let us now go back to the vortex system (43)-(44). It will prove convenient to introduce the dimensionless parameter  $\eta = \frac{\kappa}{ev}$ . This parameter governs the transition between the pure Maxwell theory ( $\eta = 0$ ) and the pure Chern-Simons theory ( $\eta \rightarrow \infty$ ). For all values of  $\eta$  there exists a topological vortex. We already know [10], that in the large  $n$  limit the Chern-Simons vortex ( $\eta \rightarrow \infty$ ) behaves like a ring of radius  $R_V = \frac{\kappa n}{e^2 v^2}$ . The ring is the domain wall that separates the symmetric phase from the Higgs phase. For a generic Maxwell-Chern-Simons vortex, we can use the same argument of [10] to understand the large  $n$  limit. As in the pure Chern-Simons case, we still have a symmetric vacuum and a Higgs vacuum. We also have a domain wall between the two vacua and, from the analysis of the previous section, we know that the wall can support a magnetic flux. We can thus conclude that the large  $n$  limit will always be a ring-like structure made of the domain wall. A stabilization computation using formula (51) gives the correct tension for the vortex.

For the pure Abrikosov-Nielsen-Olesen vortex, the behavior in the large  $n$  limit is completely different [6]: it becomes a disc of radius  $R_V = \frac{\sqrt{2n}}{ev}$  with the magnetic flux uniformly distributed inside (Fig. 13). We now want to understand the transition between these two different regimes. Since we can interpolate smoothly between pure Chern-Simons and pure Maxwell theory by changing the parameter  $\eta$ , it must certainly be possible to smoothly interpolate between the disc ( $R_V \propto \sqrt{n}$ ) and the ring ( $R_V \propto n$ ) phases.

As already mentioned, it is quite difficult to attack the problem of the large  $n$  MCS vortex numerically. To (re)construct the phase diagram  $(\eta, n)$  we have to use some intuition and extrapolate from the previous results of the domain wall with magnetic flux. In the very large  $n$  limit, the vortex always becomes a domain wall-ring. The discussion (13)-(16) done for the pure Chern-Simons vortex, follows unchanged for the MCS wall of (51) (see Figure 12).

The interesting thing happens for sufficiently small  $\eta$ , when the theory is almost Maxwell and the Chern-Simons photon mass is very small compared to the other scales of the theory. We want to consider what happens to the vortex in this region, small  $\eta$  and progressively larger  $n$ .

In the first stage, the vortex behaves like an ANO-type vortex (see Figure 13). The radius grows like  $R_V = \frac{\sqrt{2n}}{ev}$ , such that the area is linear in  $n$  and the magnetic flux is uniform inside the disc. At the edge of the disc there is a transition between the internal Coulomb phase and the external Higgs vacuum. The thickness of this transition is of order of the inverse Higgs photon mass  $1/(ev)$ . The real scalar field  $N$  essentially remains zero at this

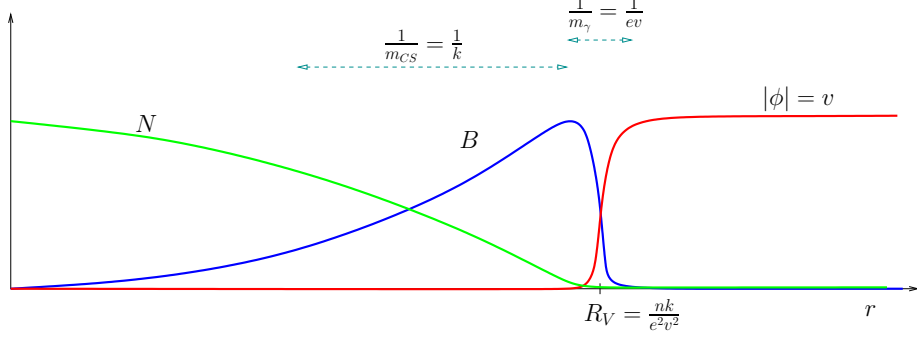


Figure 12: A sketch of the profile functions of the vortices in the CS-ring phase. The magnetic field will have an exponential from the ring, where the size of the ring is the inverse photon mass  $1/\kappa$ . The approximate profile of the magnetic field is  $B = ev^2 e^{\kappa(r-R_V)}$  while  $N = ev^2 (1 - e^{\kappa(r-R_V)}) / \kappa$ .

first stage.

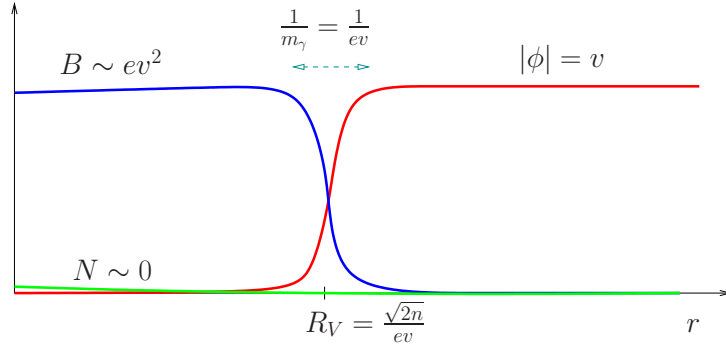


Figure 13: The profile functions of the vortices in the ANO-disc phase. The magnetic field is a plateau making up the flux tube. The field  $N$  is almost zero in this phase.

When the radius of the vortex becomes sufficiently large, reaching the inverse of the mass of the Chern-Simons photon,  $1/\kappa$ , the  $B$  and  $N$  profiles start to develop exponential tails due to the topological mass. We are entering a transition region between the ANO-type and the CS-type behavior.

Thus, we can find the ANO-like vortex “upper bound” by comparing the radius of the ANO vortex  $R = \frac{\sqrt{2n}}{ev}$  with the inverse of the CS photon mass, which is  $1/\kappa$ . The CS-like “lower bound”, however, can be found by comparing the radius of the CS vortex  $R = \frac{\kappa n}{e^2 v^2}$  with  $1/\kappa$

$$n_{\text{ANO upper}} = \frac{1}{2\eta^2}, \quad n_{\text{CS lower}} = \frac{1}{\eta^2}. \quad (54)$$

The phase diagram is shown in Figure 14.

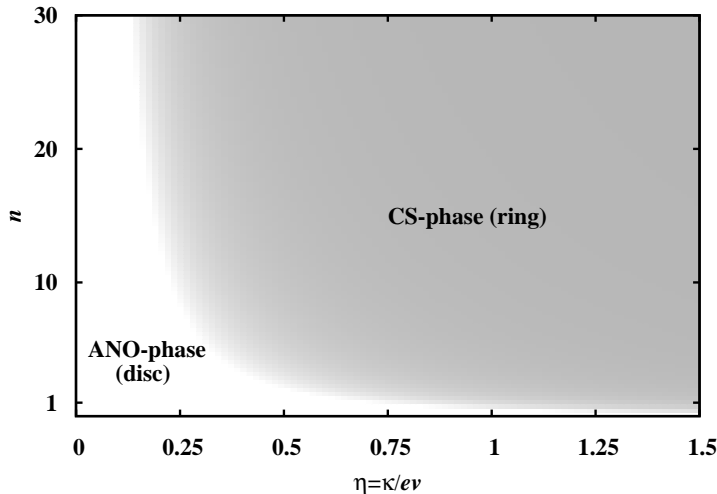


Figure 14: A phase diagram for the MCS vortex. The ANO-type phase and the CS-type phase can be separated by the curves  $n = 1/(2\eta^2)$  and  $n = 1/\eta^2$ . The transition is a smooth transition as illustrated by the tone.

## 4 Conclusions and Further Developments

Firstly, we have shown explicitly, using numerical tools, that in the large flux limit, Chern-Simons vortices approach closed domain walls. Next, we have considered the behavior of Chern-Simons vortices with a general non-BPS potential. Interesting potentials can provide stabilization for vortices with an arbitrary number, which we denote  $n_0$ , of magnetic fluxes. This phenomenon is new from the point of view of the ordinary ANO vortex, where only type I and type II behaviors are possible. We could tentatively denote this behavior a type III vortex. The interesting point is that, in principle, it could be detectable, as it resembles the physics of a type II superconductor, but with the flux tubes being physically bigger. Furthermore, it could be a nice playing ground for studying vortex interactions experimentally. We should emphasize once more, that the configurations need 2 spatial dimensions and most likely complicates the experiment and thus it could be a challenge for the nanotechnological scene.

Secondly, we have studied the Maxwell-Chern-Simons domain wall, which we conjecture to resemble the vortex in the large flux limit. With this at hand, we have shown a smooth interpolation between the Chern-Simons vortex and the ANO vortex, in the large magnetic flux limit.



There are some interesting lines of future research and generalizations of these results. One is to consider the non-Abelian generalization of Chern-Simons solitons. Recently [16], it has been shown that a non-Abelian generalization of the Chern-Simons-Higgs system gives the possibility of internal degrees of freedom living on the vortex. It would be interesting to explore also in this case the relation between the domain wall and the vortices with large flux. It would also be interesting to consider the addition of a Yang-Mills term and hence study the continuous interpolation between the two models, pure Chern-Simons [16] and pure Yang-Mills [17]. Another interesting line of research is the string-theoretical realization of Chern-Simons solitons [18]. Again it would be interesting to understand the large  $n$  behavior in this setup. Also interesting are the non-commutative geometry realizations of vortices, and in particular the “puffed” solution of ref. [19].

## Acknowledgments

S.B.G. would like to thank Minoru Eto, Kenichi Konishi and Walter Vinci for fruitful discussions. The work of S.B. is supported by DOE grant DOE/DE-FG02-94ER40823.

## References

- [1] F. Wilczek, “Fractional statistics and anyon superconductivity,” *Singapore: World Scientific (1990)* 447 p
- [2] Z. F. Ezawa, “Quantum Hall Effects,” *World Scientific (2000)* 532 p
- [3] S. C. Zhang, T. H. Hansson and S. Kivelson, “An effective field theory model for the fractional quantum hall effect,” *Phys. Rev. Lett.* **62**, 82 (1988).
- [4] A. Abrikosov, *Sov. Phys. JETP* **32** 1442 (1957)  
H. Nielsen and P. Olesen, *Nucl. Phys.* **B61** 45 (1973)
- [5] E. B. Bogomolny, “Stability Of Classical Solutions,” *Sov. J. Nucl. Phys.* **24**, 449 (1976) [*Yad. Fiz.* **24**, 861 (1976)].
- [6] S. Bolognesi, “Domain walls and flux tubes,” *Nucl. Phys. B* **730**, 127 (2005) [arXiv:hep-th/0507273]; “Large  $N$ ,  $Z(N)$  strings and bag models,” *Nucl. Phys. B* **730**, 150 (2005) [arXiv:hep-th/0507286].

- [7] S. Bolognesi and S. B. Gudnason, “Multi-vortices are wall vortices: A numerical proof,” Nucl. Phys. B **741**, 1 (2006) [arXiv:hep-th/0512132]. S. Bolognesi and S. B. Gudnason, “Soliton junctions in the large magnetic flux limit,” Nucl. Phys. B **754**, 293 (2006) [arXiv:hep-th/0606065].
- [8] S. Bolognesi, “Multi-monopoles, magnetic bags, Bions and the monopole cosmological problem,” Nucl. Phys. B **752**, 93 (2006) [arXiv:hep-th/0512133].
- [9] R. Jackiw and E. J. Weinberg, “Selfdual Chern-Simons Vortices,” Phys. Rev. Lett. **64**, 2234 (1990). J. Hong, Y. Kim and P. Y. Pac, “On The Multivortex Solutions Of The Abelian Chern-Simons-Higgs Theory,” Phys. Rev. Lett. **64**, 2230 (1990). J. Burzlaff, A. Chakrabarti and D. H. Tchrakian, “Generalized Selfdual Chern-Simons Vortices,” Phys. Lett. B **293**, 127 (1992). Y. Kim and K. M. Lee, “Vortex dynamics in selfdual Chern-Simons Higgs systems,” Phys. Rev. D **49**, 2041 (1994) [arXiv:hep-th/9211035].
- [10] R. Jackiw, K. M. Lee and E. J. Weinberg, “Selfdual Chern-Simons solitons,” Phys. Rev. D **42**, 3488 (1990).
- [11] H. c. Kao, K. M. Lee and T. Lee, Phys. Rev. D **55**, 6447 (1997) [arXiv:hep-th/9612183].
- [12] C. k. Lee, K. M. Lee and H. Min, “Selfdual Maxwell Chern-Simons solitons,” Phys. Lett. B **252**, 79 (1990). B. H. Lee, C. k. Lee and H. Min, “Supersymmetric Chern-Simons vortex systems and fermion zero modes,” Phys. Rev. D **45**, 4588 (1992).
- [13] G. V. Dunne, “Aspects of Chern-Simons theory,” arXiv:hep-th/9902115.
- [14] R. Banerjee and P. Mukherjee, “Spin of Chern-Simons vortices,” Nucl. Phys. B **478**, 235 (1996) [arXiv:hep-th/9605226]. R. Banerjee and P. Mukherjee, “Some comments on the spin of the Chern-Simons vortices,” Prog. Theor. Phys. **101**, 1189 (1999) [arXiv:hep-th/9905082].
- [15] R. Auzzi, M. Eto and W. Vinci, “Type I Non-Abelian Superconductors in Supersymmetric Gauge Theories,” arXiv:0709.1910 [hep-th].
- [16] L. G. Aldrovandi and F. A. Schaposnik, “Non-Abelian vortices in Chern-Simons theories and their induced effective theory,” arXiv:hep-th/0702209. G. S. Lozano, D. Marques, E. F. Moreno and F. A. Schaposnik, “Non-Abelian Chern-Simons vortices,” arXiv:0704.2224 [hep-th].

- [17] R. Auzzi, S. Bolognesi, J. Evslin, K. Konishi and A. Yung, “Non-abelian superconductors: Vortices and confinement in  $N = 2$  SQCD,” Nucl. Phys. B **673**, 187 (2003) [arXiv:hep-th/0307287]. A. Hanany and D. Tong, “Vortices, instantons and branes,” JHEP **0307**, 037 (2003) [arXiv:hep-th/0306150].
- [18] B. H. Lee, H. j. Lee, N. Ohta and H. S. Yang, “Maxwell Chern-Simons solitons from type IIB string theory,” Phys. Rev. D **60** (1999) 106003 [arXiv:hep-th/9904181].
- [19] N. Bouatta, J. Evslin and C. Maccaferri, “Puffed Noncommutative Non-abelian Vortices,” JHEP **0704** (2007) 037 [arXiv:hep-th/0702042].